**Karaelmas Science and Engineering Journal**
Journal home page: http://fbd.beun.edu.tr
DOI: 10.7212%2Fzkufbd.v8i2.1121

**Research Article**
Received / Geliş tarihi : 22.09.2017
Accepted / Kabul tarihi : 12.10.2017

# New Algorithm for the Lid-driven Cavity Flow Problem with Boussinesq-Stokes Suspension

*Boussinesq-Stokes Süspansiyonlu Duvar (Kapak) Hareketli Akış Problemi için Yeni Bir Algoritma*

İnci Çilingir Süngü[1*], Hüseyin Demir[2]

[1]Department of Mathematics and Science Education, Education Faculty, Ondokuz Mayıs University, Samsun, Turkey
[2]Department of Mathematics Engineering, Engineering and Natural Sciences Faculty, Gümüşhane University, Gümüşhane, Turkey

## Abstract

In the present investigation, a streamfunction-vorticity form for Boussinesq-Stokes liquids (with suspended particles) is suitably used to examine the problem of 2-D unsteady incompressible flow in a square cavity with moving top and bottom wall. A new algorithm is used for this form in order to compute the numerical solutions for high Reynolds numbers up to Re=2500. This algorithm is conducted as a combination of the multi-time-stepping temporal differential transform and the spatial finite difference methods. Convergence of the time-series solution is ensured by multi-time-stepping method. The classical benchmark results of the Newtonian liquid are recovered as a limiting case and the decelerating influence of the suspended particle on the Newtonian liquids' flow field is clearly elaborated.

**Keywords:** Differential transform-finite difference hybrid methods, Multi-time-stepping, Cavity driven flow, Numerical solution, Boussinesq-stokes liquid, Suspended particles

## Öz

Bu çalışmada Boussinesq-Stokes tipi akışkanların kapalı bölgede zamana bağlı akışı incelenmiştir. Problem, zaman değişkenine çok adımlı diferansiyel dönüşüm metodu konum değişkenlerine sonlu fark metodu uygulanarak çözülmüştür. Elde edilen zamana bağlı seri çözümünün yakınsaklığı çok adımlı metot uygulanarak sağlanmıştır. Sonuçlar, Newtonian akışkanlar için grafiklerle literatür ile karşılaştırılarak metodun etkinliği gösterilmiş, şüpheli parçacıkların Newtonian akışkanlar üzerine olan yavaşlatıcı etkisi ise grafiklerle incelenmiştir.

**Anahtar Kelimeler:** Diferansiyel dönüşüm-sonlu fark metodu, Çok adımlı metot, Çukur bölgede akış, Sayısal çözüm, Boussinesq-stokes akışkan, Şüpheli parçacıklar

## 1. Introduction

The lid-driven cavity flow problem is a well investigated one using different continua (see Ottino and Chella 1983, Tosoka and Kakuda 1994, Demir 2005, and references therein). The problem serves as a benchmark for both forced convective, free convective and mixed convective problems in a cavity of the rectangular, square, shallow and slender slot types. The paper presents the solution of the lid-driven cavity problem for a Boussinesq-Stokes liquid using a combination of the temporal differential transform and spatial finite-difference methods. The main advantage of this hybrid method is that it can be used to solve both linear and nonlinear equations without linearization. The differential transform method was used first by Zhou, 1986, who solved linear and nonlinear initial value problems in electric circuit analysis. The differential transform is an iterative procedure for obtaining analytic Taylor series solution of ordinary or partial differential equations. The method is well addressed in Chen and Liu 1998, Jang et al. 2000, Abdel-Halim Hassan 2004, Ayaz 2004, Kuo 2005. Further, the use of the multi-stepping procedure used with the differential transform method ensures the stability of the scheme leading to a convergent solution with appropriate choice of time steps. Most importantly, when solving initial-boundary-value problems, the error due to truncation produced by the finite

*Corresponding author: incicilingir@gmail.com

İnci Çilingir Süngü orcid.org/0000-0001-7788-181X
Hüseyin Demir orcid.org/0000-0002-3552-0511

difference approximation of the time derivative may become unbounded but in the case of the differential transform method it is invariably bounded if care is taken to choose $\Delta t$ as per the procedure prescribed by Jang et al. 2000. Hence, in this study we use such a hybrid method to obtain a numerical solution using an easy-to-implement iterative procedure (Chu and Chen 2008, Chu and Lo 2007, Cilingir Süngü and Demir 2012a, 2012b).

## 2. Vorticity–Streamfunction Formulation for Two-Dimensional Cavity Flow of Incompressible Boussinesq-Stokes Liquids

Following the work (Siddheshwar and Pranesh 2004), the vorticity–streamfunction formulations for the considered two-dimensional incompressible flow can be written as:

$$\frac{\partial \Omega}{\partial t}+U\frac{\partial \Omega}{\partial X}+V\frac{\partial \Omega}{\partial Y}=\frac{1}{\mathrm{Re}}\left(\frac{\partial^2 \Omega}{\partial X^2}+\frac{\partial^2 \Omega}{\partial Y^2}\right) -\frac{C}{\mathrm{Re}}\left\{\left(\frac{\partial^2}{\partial X^2}+\frac{\partial^2}{\partial Y^2}\right)^2 \Omega\right\}, \tag{1}$$

$$\Omega=\nabla^2 \Psi. \tag{2}$$

In the above equations Re is the Reynolds number, C is the couple stress parameter $\Psi$ is the stream function and $\Omega$ is the vorticity. The velocities $U$ and $V$, the stream function $\Psi$ and the vorticity $\Omega$ are related by the following equations:

$$U=-\frac{\partial \Psi}{\partial Y}, V=\frac{\partial \Psi}{\partial X}, \Omega=\frac{\partial V}{\partial X}-\frac{\partial U}{\partial Y}, \quad 0\le X\leqslant H,\ 0\le Y\le L. \tag{3}$$

The boundary conditions for the cavity problem are shown in Figure 1.

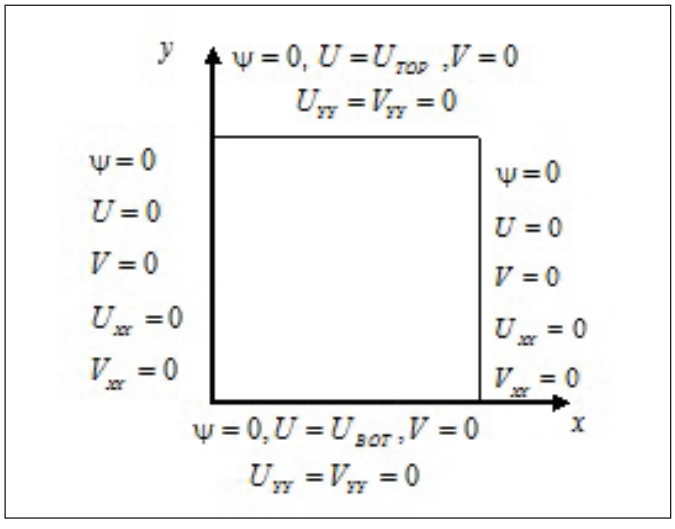


**Figure 1.** Physical configuration of the cavity problem and boundary conditions.

## 3. Numerical Algorithm Using the Temporal Differential Transform and Spatial Finite Difference Methods

In this solution technique, firstly differential transformation method is used for discretization with respect to the time variable and its derivatives. After taking differential transform of the equations, first and second order central difference formulas are used to rewrite spatial variables and their derivatives in the governing equations. Therefore, this method can combine different properties of differential transform and finite difference methods. On using the temporal differential transformation, the governing equation (1) yields the following equation:

$$\begin{aligned}&(k+1)W[x,y,k+1]+(u[x,y,k]\otimes W_x[x,y,k]\\&+v[x,y,k]\otimes W_y[x,y,k])\\&=\frac{1}{\mathrm{Re}}\left(W_{xx}[x,y,k]+W_{yy}[x,y,k]\right)-\frac{C}{\mathrm{Re}}(W_{xxxx}[x,y,k]\\&+2W_{xxyy}[x,y,k]+W_{yyyy}[x,y,k])\end{aligned} \tag{4}$$

where $k$ is parameter of differential transformation and it is a non-negative integer. $W[x,y,k]$, $u[x,y,k]$ and $v[x,y,k]$ are the differential transforms of $\Omega(x,y,t), U(x,y,t)$ and $V(x,y,t)$, respectively. The product $\otimes$ is defined as

$$\begin{aligned}&u[x,y,k]\otimes W_x[x,y,k]\\&=\sum_{l=0}^{k} u[x,y,k-l]\,W_x[x,y,l].\end{aligned} \tag{5}$$

The procedure adopted above has facilitated the conversion of the time-evolutionary equations into Poisson equations which are then solved using the central difference method. The temporal differential transform method as used in the paper takes care of stability and the finite difference method on the resulting equation results in a system of diagonally dominant linear algebraic equations (Jang et al. 2000, Cilingir Süngü and Demir 2012a, 2012b). The Gauss-Siedel iterative procedure then used to solve the linear system thus has assured convergence. To have optimized convergence rate, numerical experiments were done by using a combination of factors involving multi-time-stepping, spatial-step size and degree of the polynomial fit in time. As a result of the procedure used we have got rid of stability problems that typically arise in purely finite-difference methods (both in time and space). Since the differential transform is essentially a result emanating from the Maclaurin series, it will pose problems of convergence as a time-series solution is involved. We address this issue later on using a procedure called multi-time-stepping.

The rectangular region $R=\{(x,y)/0\le x\le H, 0\le y\le L\}$ is now discretized using a grid size of $(h_x,h_y)$. This results in the nodes $(x_i,y_j)$, where $x_i=ih_x$ and $y_j=jh_y$. We then apply the central difference approximation to the derivatives in the spatial differential equation (4). This procedure gives us the following partial difference equation that has both temporal and spatial components:

$$
\begin{aligned}
&(k+1)W[i,j,k+1]\\
&+\sum_{l=0}^{k}u[i,j,k-l]\left\{\frac{W[i+1,j,l]-W[i-1,j,l]}{2h_x}\right\}\\
&+\sum_{l=0}^{k}v[i,j,k-l]\left\{\frac{W[i,j+1,l]-W[i,j-1,l]}{2h_y}\right\}\\
&=\frac{1}{\mathrm{Re}}\left(\left\{\frac{W[i+1,j,k]-2W[i,j,k]+W[i-1,j,k]}{h_x^2}\right\}\right.\\
&\left.+\left\{\frac{W[i,j+1,k]-2W[i,j,k]+W[i-1,j,k]}{h_y^2}\right\}\right)\\
&-\frac{C}{\mathrm{Re}}\left\{\frac{1}{h_x^4}\{W[i+2,j,k]-4W[i+1,j,k]+6W[i,j,k]\right.\\
&-4W[i-1,j,k]+W[i-2,j,k]\}\\
&+\frac{2}{h_x^2h_y^2}\{W[i+1,j+1,k]-2W[i+1,j,k]+W[i+1,j-1,k]\\
&-2(W[i,j+1,k]-2W[i,j,k]+W[i,j-1,k])\\
&+W[i-1,j+1,k]-2W[i-1,j,k]+W[i-1,j-1,k]\}\\
&+\frac{1}{h_y^4}\{W[i,j+2,k]-4W[i,j+1,k]+6W[i,j,k]\\
&\left.-4W[i,j-1,k]+W[i,j-2,k]\}\right\}
\end{aligned}
$$

$$1\le i\le M-1, 1\le j\le N-1 \; and \; 0\le k\le K-1 \qquad (6)$$

The ranges of i and j are $1\le i\le M-1$ and $1\le j\le N-1$. In equation (6), $W[i,j,k]$ represents the value of $W$ at the discretized points $(x_i,y_j,t)$. To solve the partial difference equation (6) we need to know the initial and boundary conditions and these can be obtained from the no-slip and vanishing couple stress conditions depicted in Figure 1. The differential transform of the boundary conditions are:

$$
\begin{aligned}
&u[i,0,0]=U_{BOT}, v[i,0,0]=0,\\
&u[i,0,0]=0\\
&v[i,0,0]=0
\end{aligned}
,0\le i\le M, 1\le k\le K, \qquad (7)
$$

$$
\begin{aligned}
&u[i,N,0]=U_{TOP}, v[i,N,0]=0,\\
&u[i,N,k]=0\\
&u[i,N,k]=0
\end{aligned}
,0\le i\le M, 1\le k\le K. \qquad (8)
$$

## 4. Convergence and Stability Properties for New Algorithm

Having reformulated the cavity problem as an initial-boundary-value-problem involving a partial difference equation we now propose to use the multi-stepping procedure of Yu and Chen (1998) that was put to use in practical problems by Odibat et al. 2010. Using such a multi-stepping procedure we obtain an approximate solution that converges in wider time regions. We divide the time interval of interest $[0,T]$ into P subintervals, namely $[t_{p-1},t_p], p=1,2,...,P$ of equal step size $\Delta t=T/P$ by using the nodes $t_p=p\Delta t$ on the time coordinate axis. The inverse differential transform gives us the solution for $\Omega$ at the discretized points $(x_i,y_j,t)$, in each of the sub-intervals $[t_{p-1},t_p], p=1,2,...,P,$ in the form:

$$\Omega^{(p)}(x_i,y_j,t)=\sum_{k=0}^{K}W^{(p)}[i,j,k](\Delta t)^k, t\in[t_{p-1},t_p], \qquad (9)$$

where $W^{(p)}[i,j,k]$ is the differential transform of $\Omega(x_i,y_j,t)$ in the time interval $[t_{p-1},t_p]$. At this point the time step $\Delta t$ is to be chosen to keep the truncation error within a specified bound and minimize the computation time that arise in the power series solution (9).

The solution procedure is repeated until convergent solution is achieved. The tolerance value of $10^{-3}$ is used in this study. Given the tolerance, the global error in a numerical method cannot be determined, in general, the local error is related to the global error. Theoretically, if a tolerance $\varepsilon$ is given, the global error would not exceed $\varepsilon$ for any grid point (Jang et al. 2000). From error estimates of Maclaurin series, one can choose a proper grid size according to a criterion that the global error is constrained within a specified bound. Using this fact, we can choose time step to have the bound as follows:

$$\Delta t<\left(\frac{\varepsilon}{|W[i,j,K+1]|}\right)^{1/K+1}. \qquad (10)$$

## 5. Results and Discussion

The lid-driven unsteady cavity flow is solved by considering the following three cases:

(i) only the top wall moving with constant speed in the positive direction of x-axis

(ii) Both top and bottom walls moving with constant speeds in the positive direction of x-axis and

(iii) Top and bottom walls moving with constant speeds in the positive and negative directions of x-axis respectively.

Firstly, the present model is validated by flow in a square cavity because there are fairly large numbers of studies conducted for square cavity driven flow. Figures (2)-(20) illustrate the streamlines of $\psi$ for flows with Reynolds

number in the range 1<Re<2500. The grid resolution chosen is 40x40. In order to get grid-independent numerical results, in this study we employed several different grid resolutions, from 10x10 to 70x70, and found that the grid resolution 40x40 is good enough for the chosen Reynolds number range. For higher *Re*, one must choose a finer grid resolution. For low Re<1000, only one vortex appears in the cavity. For 1000<Re<2000, there is a primary one near the centre and a pair of secondary ones in the lower corners of the cavity. At *Re*>2000, a third secondary vortex is seen in the upper left corner. We can also see that the centre of the primary vortex moves toward the centre of the cavity as *Re* increases. The velocity component u along the vertical centre line for different Re is shown in Figure 2A and Figure 2B and we use the u -velocity profiles in Figure 2 to test the accuracy of the solution. These observations show that the present simulation is in agreement with the previous studies which can be seen in Figure 2C, D, E and F. According to the figures, the present simulation is in agreement with the previous studies (Tosoka and Kakuda 1994, Demir 2005). As *Re* becomes larger the profiles are found to become nearly linear in the central core of the cavity. Comparison of the efficiency of the different approaches is a very important aspect of this study. The computational time and iteration numbers for various Reynolds number using different numerical methods are documented in Table 1 and this shows that the hybrid approach is faster than the corresponding highly optimized finite difference method in two dimensional computations (Guo et al. 2000, Pozrikidis 2001, Erturk et al. 2005, Chen et al. 2008). Therefore the

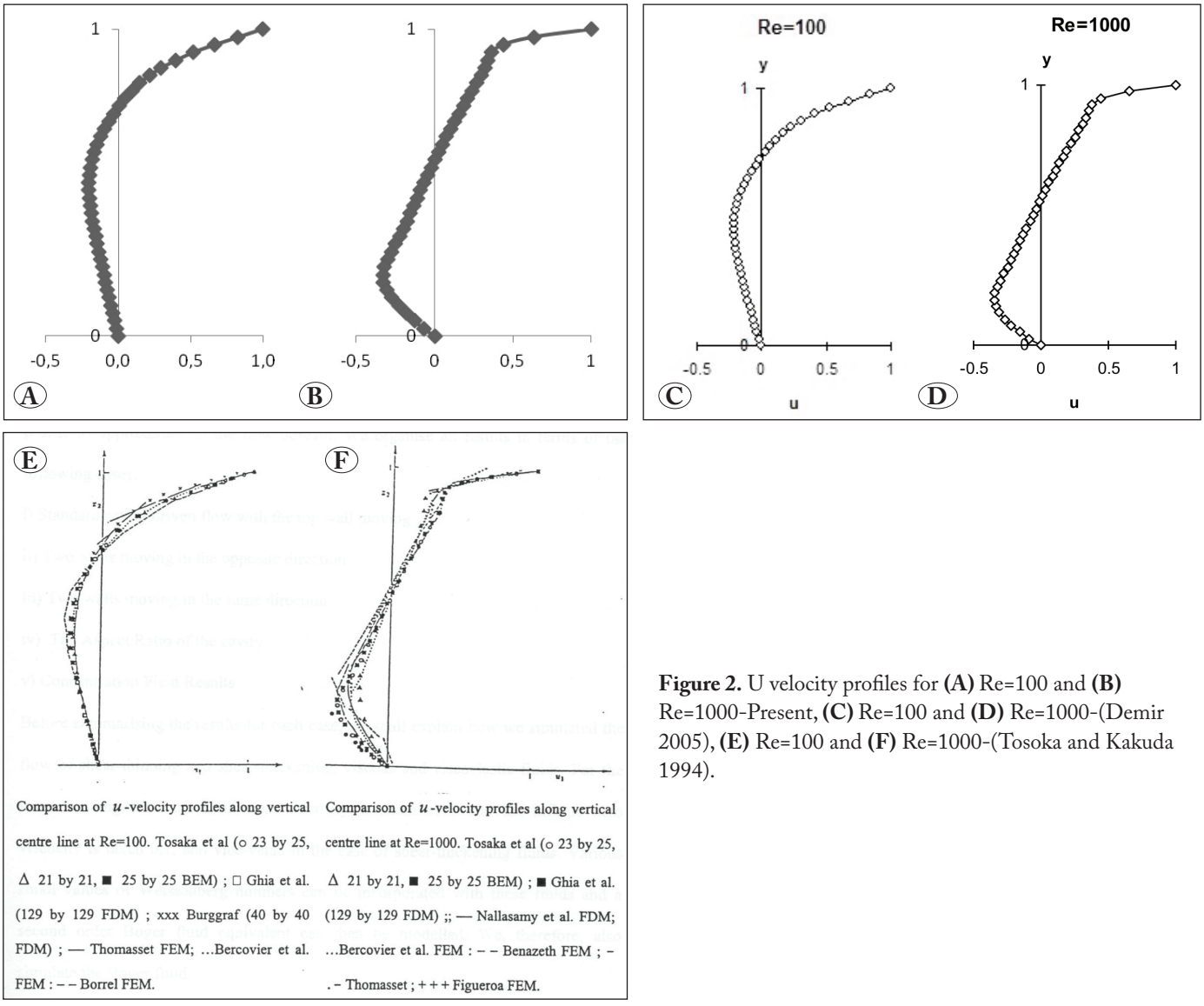


**Figure 2.** U velocity profiles for **(A)** Re=100 and **(B)** Re=1000-Present, **(C)** Re=100 and **(D)** Re=1000-(Demir 2005), **(E)** Re=100 and **(F)** Re=1000-(Tosoka and Kakuda 1994).

numerical results indicated that the proposed hybrid method constructs a simple iterative process, fast, very accurate and efficient method.

Finally, we simulated flow in a two-sided cavity driven flow. In contrast to the fairly large number of studies conducted for one-sided lid-driven cavities, relatively little investigation has been carried out for flow in a two-sided lid-driven cavity which has been employed to study mixing, drying processes, fluid dynamics as well as polymer processing and thin film coating. The top wall moves with velocity $U_{TOP}$ and the bottom wall moves in the same direction with velocity being either $U_{BOT}$ or $-U_{BOT}$. Figures (9)-(14) show the flow patterns of symmetrical driving for different Reynolds number flows. When both walls move in the same direction with the same velocity ($U_{TOP} = U_{BOT}$) the streamlines are symmetric with respect to the mid-plane of $y$ coordinate. For the two walls moving in the opposite direction ($U_{TOP} = -U_{BOT}$) the streamlines are symmetric with respect to the two main diagonals of the cavity. Comparison is made for graphical comparison in the literature and these are shown in Figure 3(B), 9(B), 15(B) and produced by Chien et al. 1986. Our results are agree very well with those qualitatively as seen in Figure 3(A), 9(A), 15(A). So far we have discussed the results of the lid-driven cavity problem involving a Newtonian liquid and gained the confidence that the proposed hybrid scheme yields equally good results as that of the purely finite-difference method adopted in works published in literature.

We now move on to discuss the effect of suspended particles on the streamlines of the lid-driven convection problem discussed so far. The streamlines in couple stress liquids are more circular than that of the Newtonian cells but the

**Table 1.** Comparison of the computational efficiency between different methods for the one-sided lid-driven square cavity flow. **A:** Guo et al. 2000; **B:** Pozrikidis 2001; **C:** Erturk et al. 2005; **D:** Chen et al. 2008; **E:** Present results

| | Re = 50 | | Re = 400 | | Re = 100 | |
|---|---|---|---|---|---|---|
| | Iterations | Time | Iterations | Time | Iterations | Time |
| A | 73900 | 921 | 89200 | 1082 | 93400 | 1139 |
| B | 2000 | 743 | 2000 | 1215 | 2000 | 1746 |
| C | 3700 | 468 | 4900 | 608 | 6300 | 767 |
| D | 2200 | 291 | 4500 | 596 | 6100 | 812 |
| E | 270 | 2.3895 | 271 | 21.7884 | 275 | 33.825 |

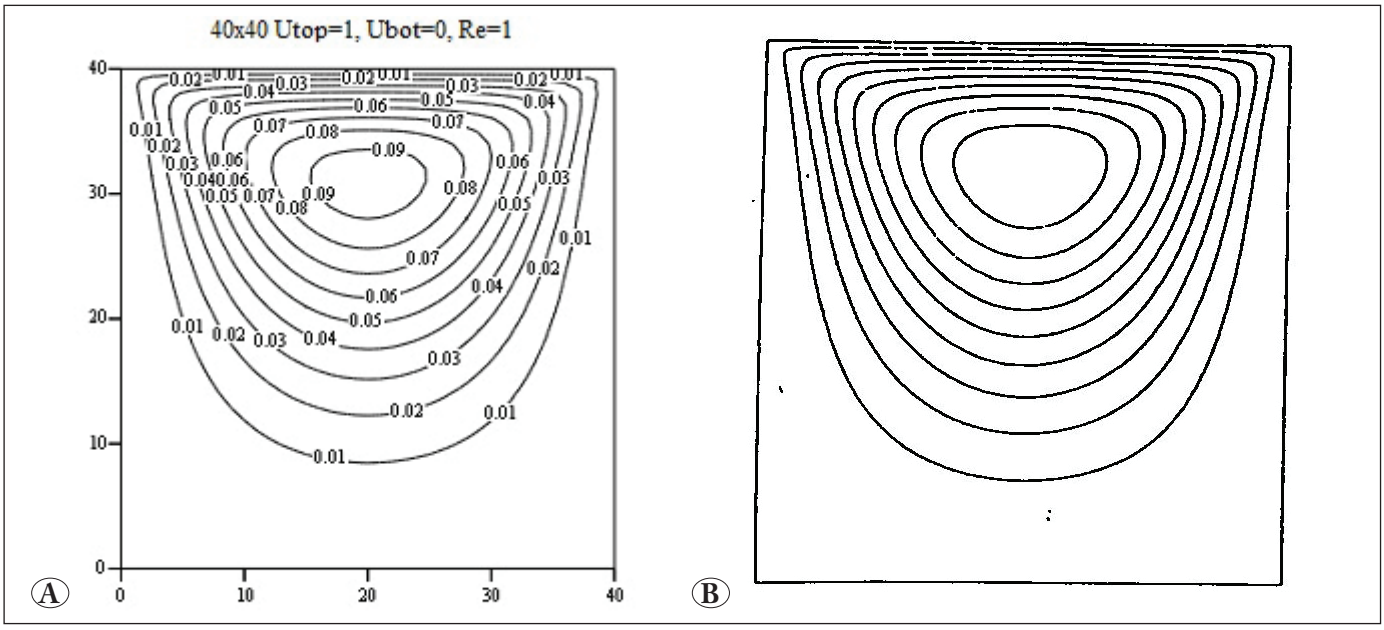


**Figure 3:** Streamlines at Re=1 for a Newtonian flow with only the top wall moving, **(A)** Present, **(B)** Chien et al. 1986.

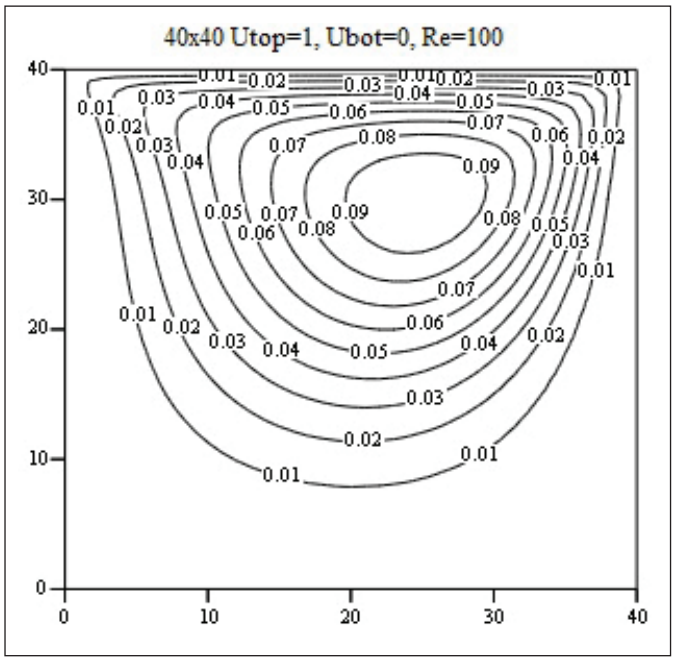


**Figure 4.** Streamlines at Re=100 for a Newtonian flow with only the top wall moving.

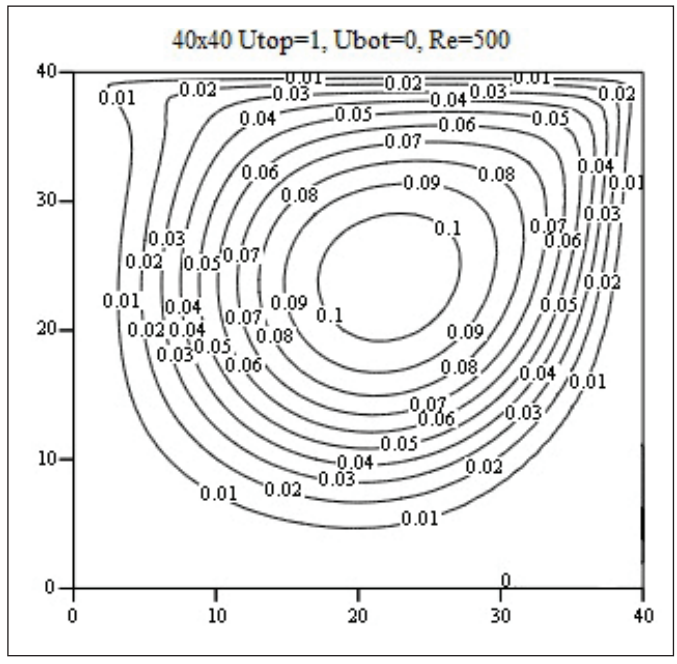


**Figure 5.** Streamlines at Re=500 for a Newtonian flow with only the top wall moving.

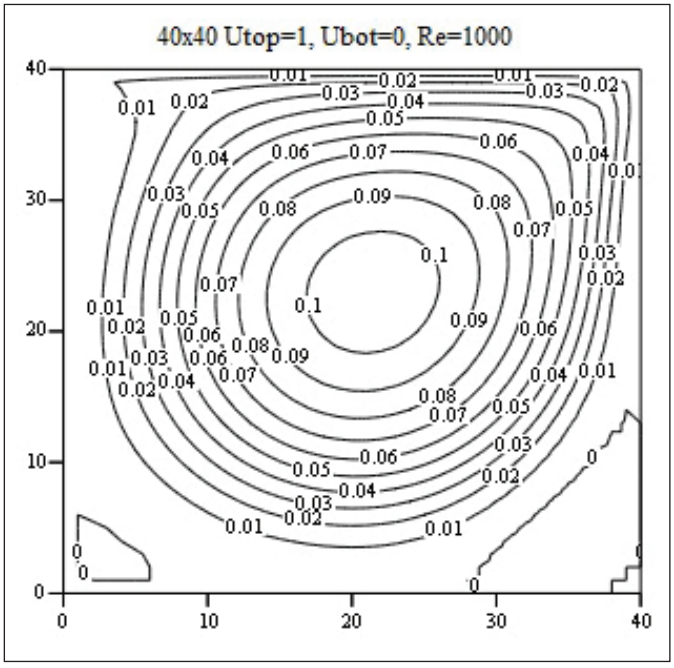


**Figure 6.** Streamlines at Re=1000 for a Newtonian flow with only the top wall moving.

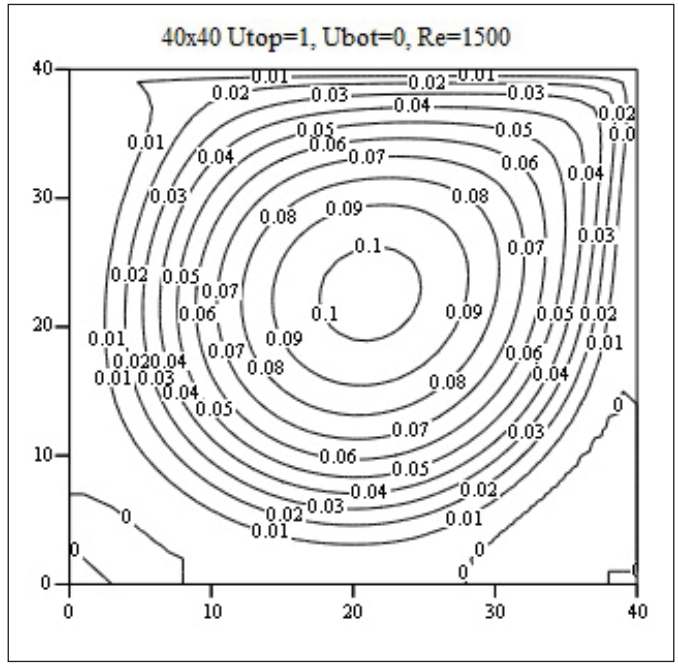


**Figure 7.** Streamlines at Re=1500 for a Newtonian flow with only the top wall moving.

behaviour of the flow with increase in *Re* is qualitatively similar in both the liquids. The reason for the circular nature of the cells in the case of couple stress liquids is that the suspended particles slow down the carrier fluid (Newtonian fluid) and by Einstein's law this can be attributed to the enhancement of viscosity due to the addition of suspended particles. The results shown in Figures 21 and 22 suggest the above results on couple stress liquids.

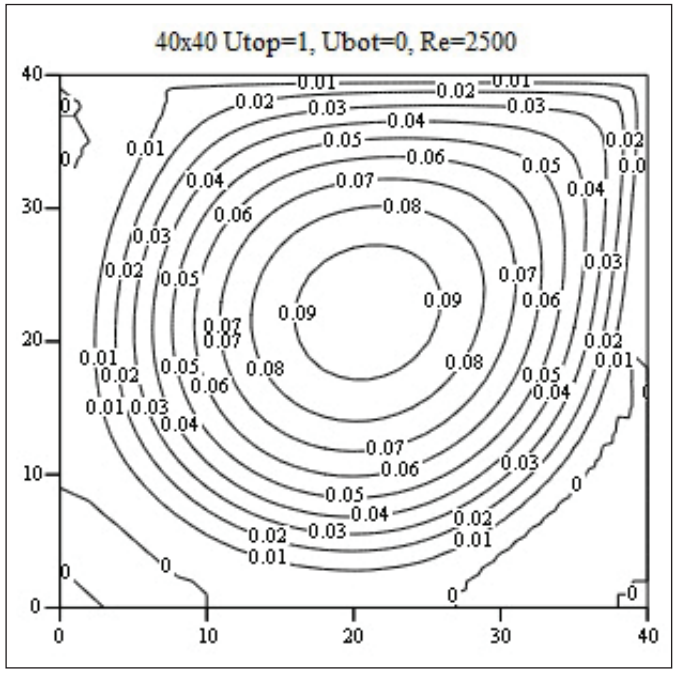


**Figure 8.** Streamlines at Re=2500 for a Newtonian flow with only the top wall moving.

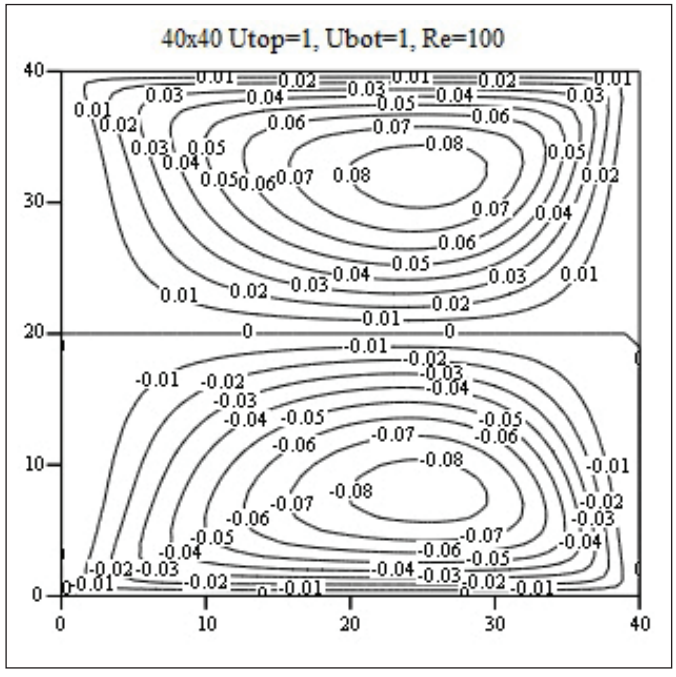


**Figure 10.** Streamlines at Re=100 for Newtonian flow when the walls move in the same direction.

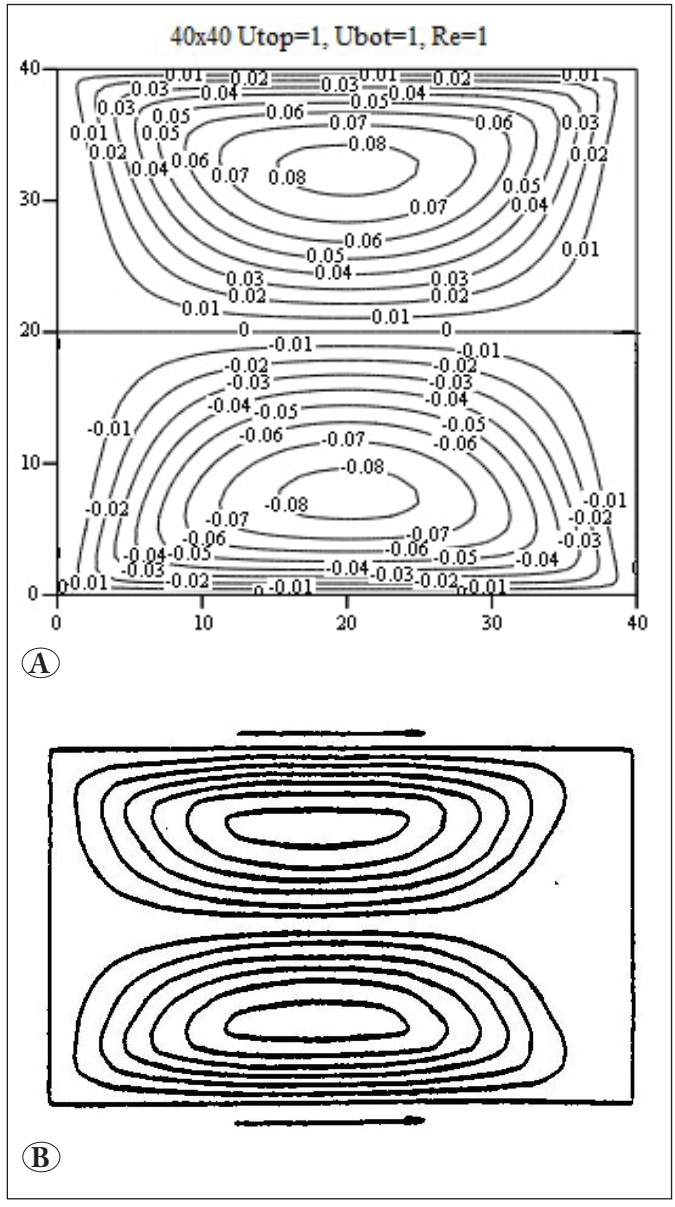


**Figure 9.** Streamlines at Re=1 for Newtonian flow when the walls move in the same direction **(A)** Present, **(B)** Chien et al. 1986.

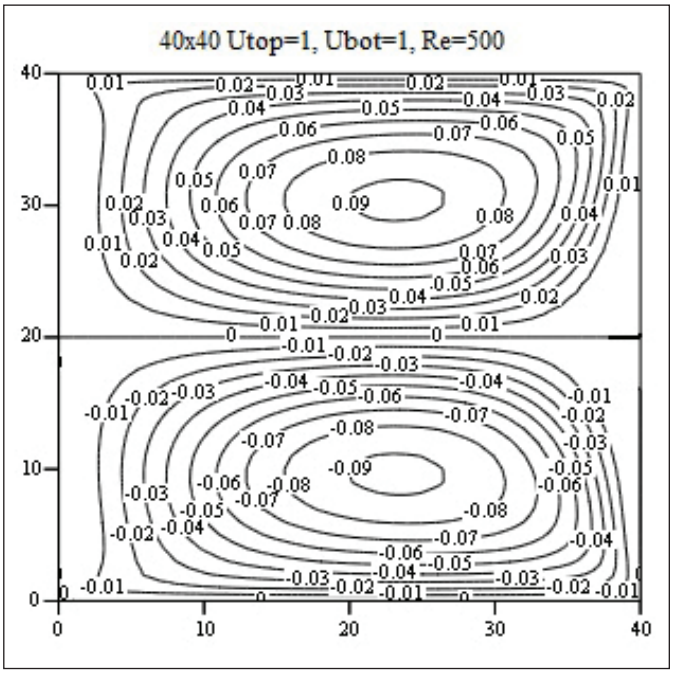


**Figure 11.** Streamlines at Re=500 for Newtonian flow when the walls move in the same direction.

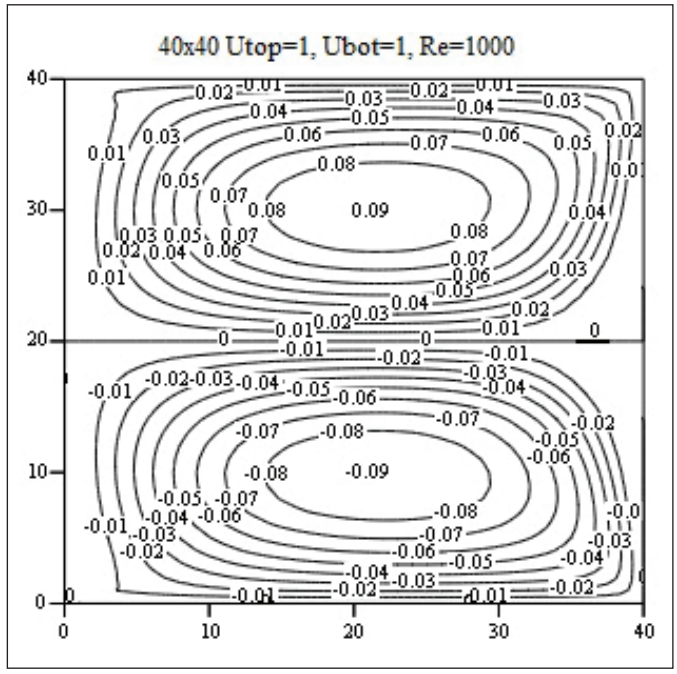


**Figure 12.** Streamlines at Re=1000 for Newtonian flow when the walls move in the same direction.

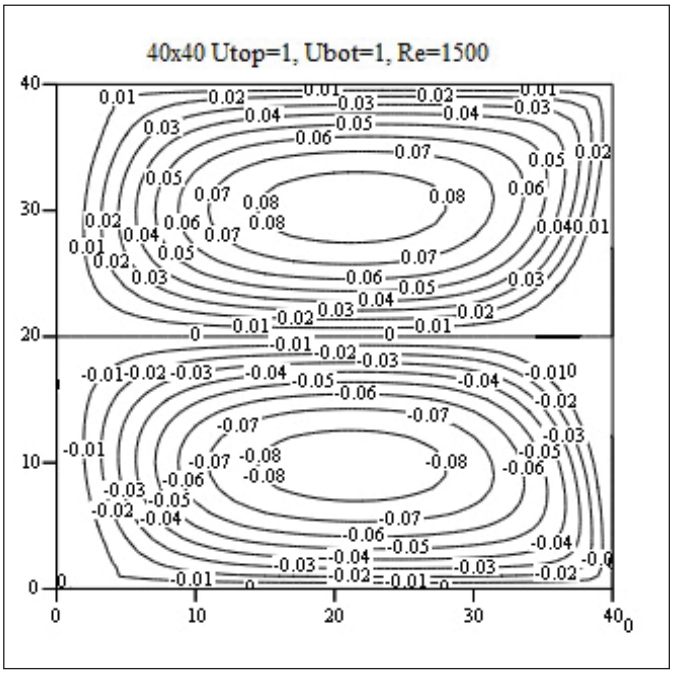


**Figure 13.** Streamlines at Re=1500 for Newtonian flow when the walls move in the same direction.

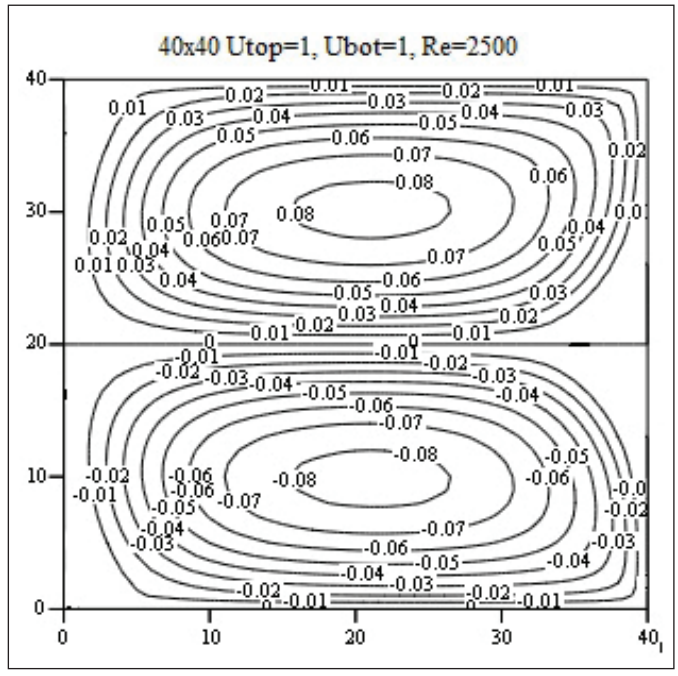


**Figure 14:** Streamlines at Re=2500 for Newtonian flow when the walls move in the same direction.

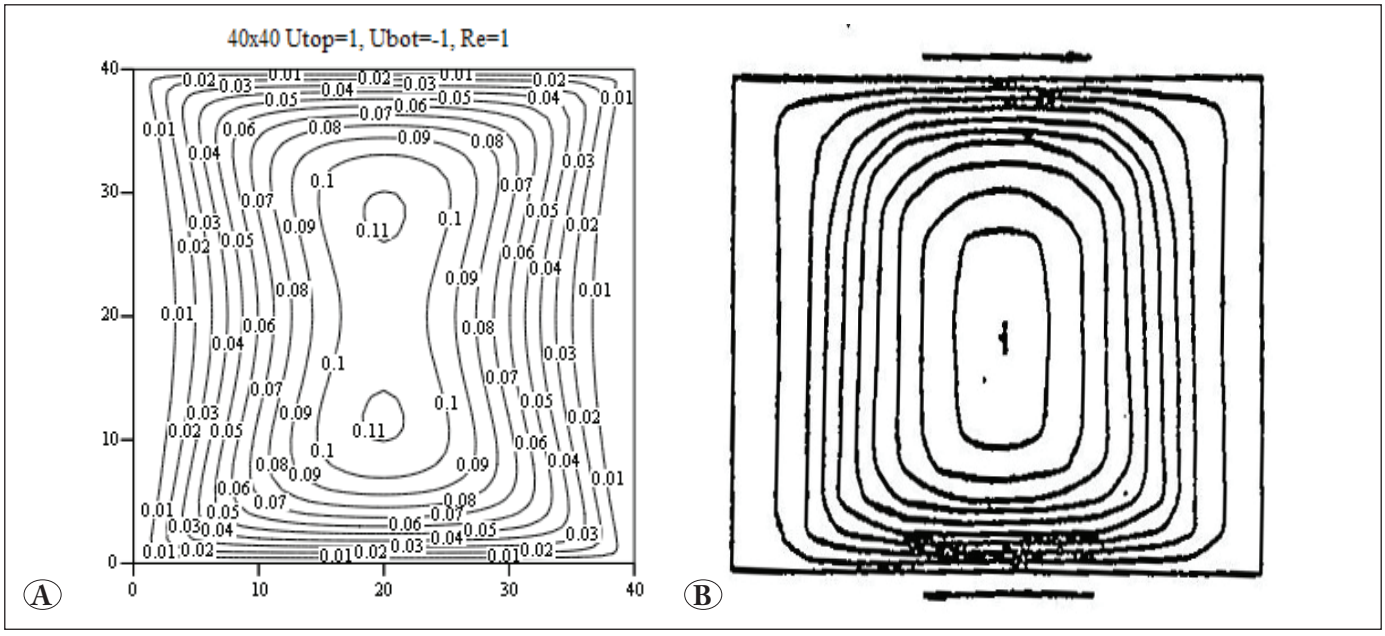


**Figure 15.** Streamlines at Re=1 for Newtonian flow for walls moving in the opposite direction, **(A)** Present, **(B)** Chien et al. 1986.

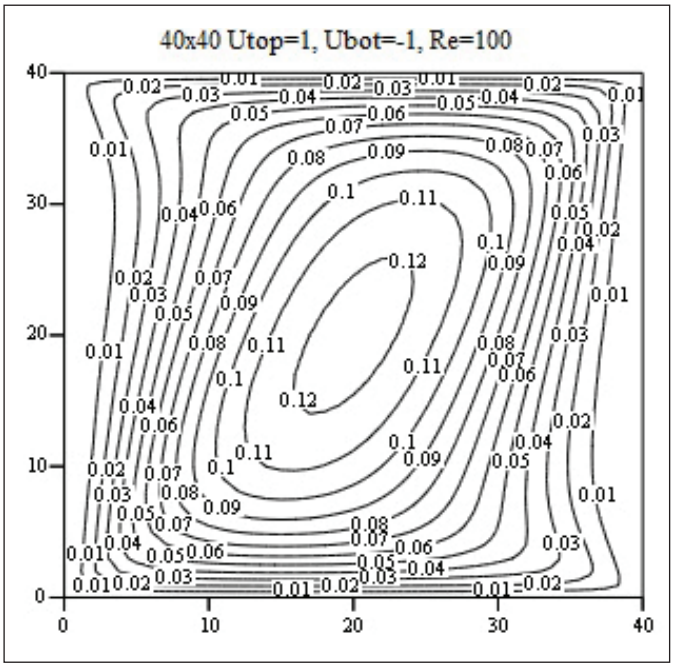


**Figure 16.** Streamlines at Re=100 for Newtonian flow for walls moving in the opposite direction.

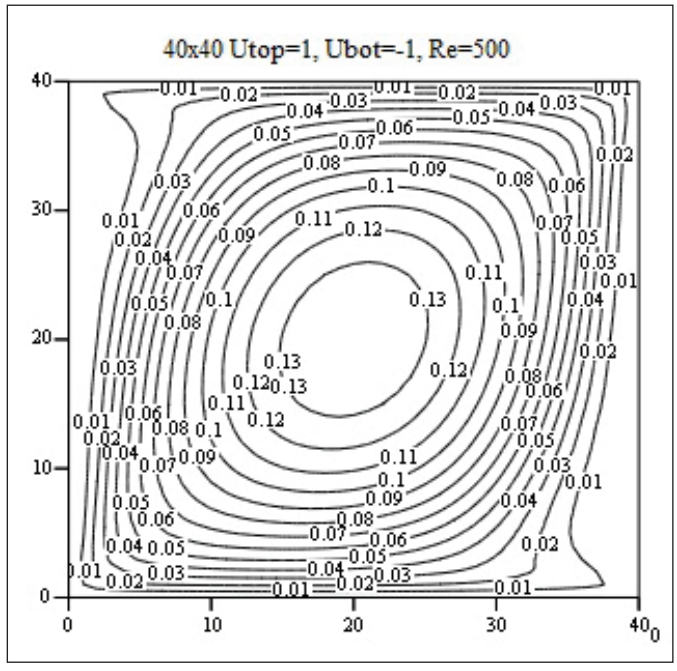


**Figure 17.** Streamlines at Re=500 for Newtonian flow for walls moving in the opposite direction.

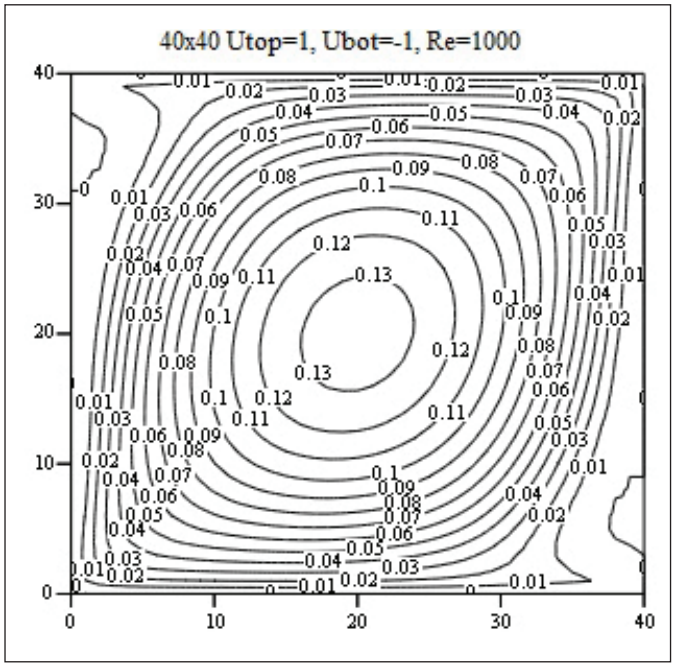


**Figure 18.** Streamlines at Re=1000 for Newtonian flow for walls moving in the opposite direction.

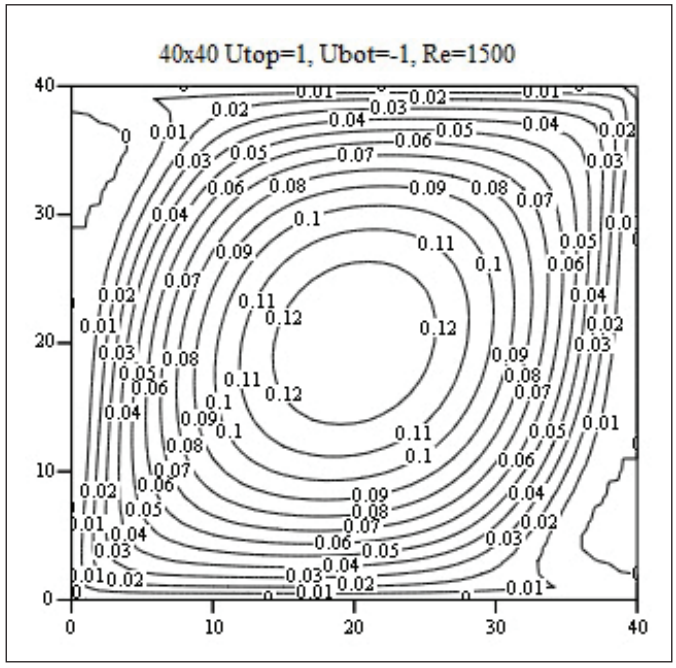


**Figure 19.** Streamlines at Re=1500 for Newtonian flow for walls moving in the opposite direction.

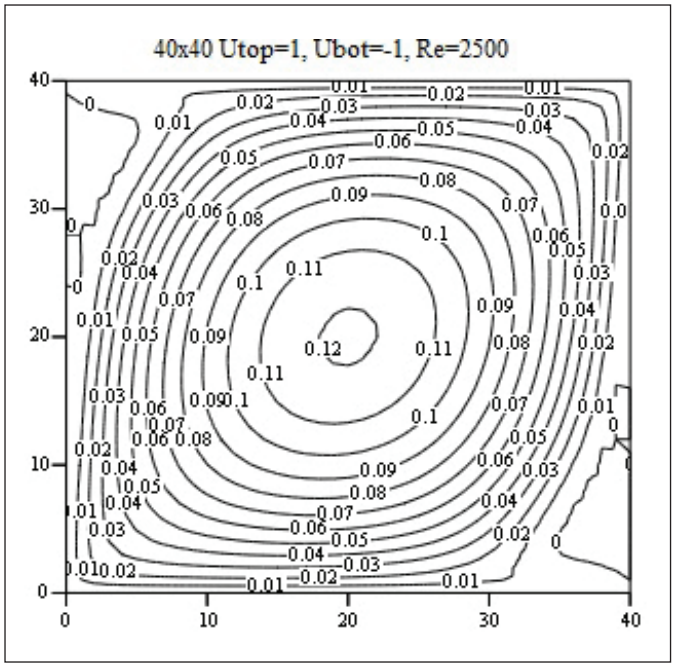


**Figure 20.** Streamlines at Re=2500 for Newtonian flow for walls moving in the opposite direction.

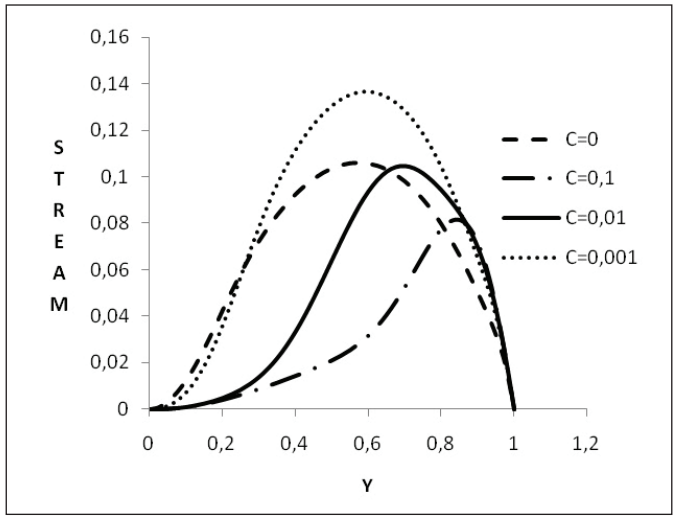


**Figure 21.** Stream function values along vertical centre line at Re=1000 for different C.

## 6. Conclusion

The study achieved the objective of examining and validating a new hybrid numerical method of solving the lid-driven cavity problem. The proposed hybrid method is shown to yield a convergent solution and does not seem to have limitations in handling any upper-limit of Reynolds Number and may be an important tool to reduce the execution time and memory requirements for large scale computations and get remarkable results in predicting the solutions of lid driven square cavity flow problems. The results are found acceptable for both quantitatively and qualitatively in case of Newtonian fluids without and with suspended particles. The works on other types of continua are in progress.

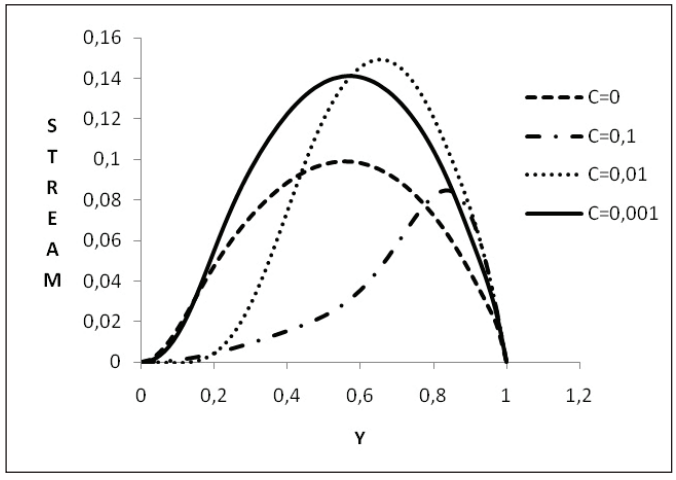


**Figure 22.** Stream function values along vertical line at Re=2000 for different C.

## 7. References

**Abdel-Halim Hassan, IH. 2004.** Differential transform technique for solving higher order initial value problems. *Appl. Math. Comput.*, 154: 299-311.

**Ayaz, F. 2004.** Solutions of the system of differential equations by differential transform method. *Appl. Math. Comput.*, 147: 547-567.

**Chen, CL., Liu YC. 1998.** Solution of two-point boundary-value problems using the differential transformation method. *J. Optim. Theory App.*, 99: 23-35.

**Chen, S., Tölke, J., Krafczyk, M. 2008.** A new method for the numerical solution of vorticity-streamfunction formulations. *Comput.. Methods Appl. Mech. En.*, 198: 367-376.

**Chien, WL., Rising, H., Ottino, JM., 1986.** Laminar mixing and chaotic mixing in several cavity flows. *J. Fluid. Mech.*, 170: 355-377.

**Chu, HP., Chen, CL. 2008.** Hybrid differential transform and finite difference method to solve the nonlinear heat conduction problem. *Commun. Nonlinear Sci. Numer. Simul.*, 13: 1605-1614.

**Chu, HP., Lo, CY., 2007.** Application of the hybrid differential transform –finite difference method to nonlinear transient heat conduction problems. *Numer. Heat Tr. A-Appl.*, 53(3): 295-307.

**Cilingir Süngü, I., Demir, H., 2012a.** Solutions of the system of differential equations by differential transform/finite difference method. *Nwsa-Phys. Sci.*, 7(2): 66-73.

**Cilingir Süngü, I., Demir, H. 2012b.** Application of the hybrid differential transform method to the nonlinear equations *A.M. Scirp.*, 3: 246-250.

**Demir, H. 2005.** Numerical modelling of viscoelastic cavity driven flow using finite difference simulations. *Appl. Math. Comput.*, 166: 64-83.

**Erturk, E., Corke, TC., Gokcol, C. 2005.** Numerical solutions of 2-d steady incompressible driven cavity flow at high reynolds numbers. *J. Numer.. Meth. Fluids*, 48: 747-774.

**Guo, ZL., Shi, BC., Wang, NC. 2000.** Lattice bgk model for incompressible navier-stokes equation. *J. Comput. Phys.*, 165: 288-306.

**Jang, MJ., Chen, CH., Liy, YC. 2000.** On solving the initial value problems using the differential transform method. *Appl. Math. Comput.*, 115: 145-160.

**Kuo, BL. 2005.** Applications of the differential transform method to the solutions of the free convection problem. *Appl. Math. Comput.*, 165: 63-79.

**Odibat, ZM., Bertelle, C., Aziz-Alaoui, MA., Duchamp, GHE. 2010.** A multi-step differential transform method and application to non-chaotic systems. *Comput. Math. Appl.*, 59: 1462-1472.

**Ottino, JM., Chella, R., 1983.** Laminar mixing of polymetric liquids: a brief review and recent theoretical developments. *Polym. Eng. Sci.*, 23: 357-379.

**Pozrikidis, C. 2001.** Fluid Dynamics: Theory, Computation and Numerical Simulation. *Accompanied by the Software Library FDLIB*, Kluwer (Springer), Heidelberg, Berlin, New York. http://dehesa.freeshell.org/FDLIB/fdlib.shtml

**Siddheshwar, PG., Pranesh, S. 2004.** An analytical study of linear and nonlinear convection in boussinesq-stokes suspensions. *Int. J. Nonlinear Mech.*, 39(1):165-172.

**Tosoka, N., Kakuda, K. 1994.** Development of BEM for convective viscous flow problems, *Int. J. Solid Struc.*, 31: 1847-1859.

**Yu, LT., Chen, CK. 1998.** The solution of the Blasius equation by the differential transformation method. *Math. Comput. Model.*, 28: 101-111.

**Zhou, JK. 1986.** Differential transformation and its applications for electrical circuits, Huazhong University Press, Wuhan, P. R. China, In Chinese.